

# Carbonylative Sonogashira Coupling in the Synthesis of Ynones: A Study of “Boomerang” Phenomena

Marie Genelot,<sup>a,b</sup> Véronique Dufaud,<sup>b,c,\*</sup> and Laurent Djakovitch<sup>a,\*</sup>

<sup>a</sup> Université de Lyon, CNRS, UMR 5256, IRCÉLYON, Institut de recherches sur la catalyse et l'environnement de Lyon, 2 avenue Albert Einstein, F-69626 Villeurbanne, France

Fax: (+33)-4-7244-5399; phone: (+33)-4-7244-5381; e-mail: Laurent.Djakovitch@ircelyon.univ-lyon1.fr

<sup>b</sup> Université de Lyon, CNRS, UMR 5182, Laboratoire de Chimie, Ecole Normale Supérieure de Lyon, 46 Allée d'Italie, F-69364 Lyon Cedex 07, France

<sup>c</sup> Present address: Université de Lyon, Laboratoire de Chimie, Catalyse, Polymère, Procédés (C2P2), 43 Bd du 11 novembre 1918, 69616 Villeurbanne cedex, France

Fax: (+33)-4-7243 1795; phone: (+33)-4-7243-1792; e-mail: veronique.dufaud@univ-lyon1.fr

Received: April 26, 2013; Revised: July 4, 2013; Published online: ■ ■ ■, 0000



Supporting information for this article is available on the WWW under <http://dx.doi.org/10.1002/adsc.201300357>.

**Abstract:** The behaviour of several organophosphino-palladium complexes immobilized on mesoporous silica during the palladium-catalyzed synthesis of propynone by carbonylative Sonogashira coupling was studied, particularly concerning leaching/redeposition phenomena. The results demonstrated that this cross-coupling reaction is catalyzed by soluble species. Furthermore, it is shown that the palladium leaching is not initiated by the oxidative addition step but rather by palladium-decoordination from grafted ligand. Despite this decoordination, catalyst performance after recycling is adequate. Additionally, several parameters linked either to catalyst prepa-

ration or reaction procedures were shown to reduce leaching allowing one to achieve metal contamination levels close to the recommendation of the European Agency for the Evaluation of Medicinal Products. Interestingly, this heterogeneous palladium-catalyzed procedure is fully selective toward the formation of ynones, allowing the preparation of various target compounds.

**Keywords:** boomerang phenomena; carbonylative Sonogashira cross-coupling; leaching/redeposition phenomena; mesoporous silica; SBA-15 and SBA-3 palladium catalysts; ynones

## Introduction

Ynones represent attractive structures due to their numerous biological properties.<sup>[1]</sup> Additionally, they are also widely used as key intermediates for the synthesis of natural compounds,<sup>[2]</sup> pharmaceuticals,<sup>[3,4]</sup> or more generally, various heterocycles.<sup>[5–8]</sup> Among the different pathways described for their synthesis, the carbonylative Sonogashira cross-coupling has emerged as a powerful tool to access this class of compounds. Indeed, this reaction allows for the one-step formation of ynones starting from three simple (available) reagents: an aryl or alkyl halide, a terminal alkyne and carbon monoxide. During the last three decades, numerous modifications of the original work of Tanaka<sup>[9]</sup> have been made. The solvent has been the object of studies oriented toward greener processes by, for example, using of ionic liquid<sup>[10,11]</sup> to enable recycling of the catalytic system, or the use of greener solvents such as water.<sup>[12,13]</sup> Other improvements gen-

erally concern the bases that are often linked to solvent modifications. Thus, although triethylamine remains the most commonly used, inorganic and water-compatible bases such as potassium carbonate<sup>[14]</sup> and ammonia<sup>[15]</sup> have also been employed. In addition, reaction times have been decreased by microwave heating,<sup>[16]</sup> temperature and pressure have been lowered<sup>[12]</sup> and microflow reactors<sup>[17]</sup> have also been developed to work at atmospheric pressure of carbon monoxide, to name just a few examples. The most investigated aspect is the modification of the catalytic system either by the adjustment of the metal catalyst (palladium, copper,<sup>[18]</sup> or a combination of both<sup>[14,19]</sup>) or the use of different ligands,<sup>[10,16,20]</sup> the choice being generally dictated by the reactivity of the targeted substrates.<sup>[15]</sup> Heterogeneous catalysts have also been developed using either commercially available Pd/C<sup>[21]</sup> or custom catalysts such as magnetically separable Pd/Fe<sub>3</sub>O<sub>4</sub><sup>[22]</sup> or Pd complexes grafted onto MCM-41 silica<sup>[23]</sup>.

In the course of our studies toward the Pd-catalyzed multi-step synthesis of 4-quinolones from iodoanilines and alkynes under a carbon monoxide atmosphere,<sup>[24–27]</sup> various heterogeneous Pd catalysts prepared by grafting onto SBA-15 type silica were evaluated. In this approach, ynones represent key intermediates; therefore developing Pd catalysts based on mesoporous supports particularly retained our attention. Ynones can also either be active compounds or useful intermediates to access biologically active molecules, thus metallic contamination of the product is of particular concern. Indeed, the European specifications regarding metal contamination in medically relevant products are quite low as only 1 ppm of palladium are recommended for a parenteral administration of the active molecule.<sup>[28]</sup> It should be easier to reach such a low palladium contamination limit using solid, heterogeneous catalysts rather than homogeneous ones (ease of separation, recovery and recycling).

Given that the metal contamination issue is generally related to leaching of active metal species from the support, we were surprised to find only sporadic reports dealing with this point for the carbonylative Sonogashira coupling while it has been intensively studied for other Pd-catalyzed couplings such as Sonogashira,<sup>[29–31]</sup> Suzuki<sup>[32–48]</sup> or Heck<sup>[32,37,39,41,49–71]</sup> reactions.

Thus, we decided to undertake studies on the synthesis of ynones using various heterogeneous Pd catalysts, focusing our attention on leaching and redeposition of Pd species from and to the support (the so-called “boomerang effect”). Different parameters influencing those phenomena were evaluated in order to reduce the final palladium contamination. Herein, we describe the results of these studies enhanced by kinetic experiments, comparing different types of heterogeneous Pd catalysts to a homogeneous Pd complex in the carbonylative Sonogashira coupling.

## Results and Discussion

### Preparation of Palladium Catalysts

Four heterogeneous Pd catalysts based on SBA type silica materials were prepared and evaluated in this study. The results were compared to those obtained with a homogeneous Pd catalyst, namely  $[\text{PdCl}_2(\text{dppp})]$  (with  $\text{dppp}$  = diphenylphosphinopropane), which, according to previous results,<sup>[24]</sup> was found to be very selective for this transformation.

In order to investigate the influence of the structural features of the Pd complex toward leaching, we choose three Pd complexes differing by the nature of the phosphine ligands and the degree of linkage to the solid surface. These include two complexes with monodentate phosphine ligands varying by the elec-

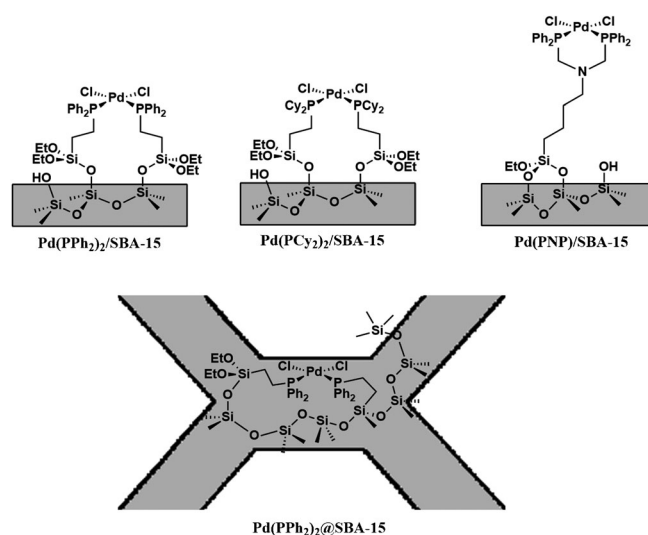


**Figure 1.** Targeted Pd hybrid catalysts.

tronic and steric properties, namely Alkyl- $\text{PPh}_2$  and Alkyl- $\text{PCy}_2$ . A third Pd complex bearing a bidentate phosphine ligand, namely Alkyl- $\text{N}(\text{CH}_2\text{PPh}_2)_2$  was also selected. These complexes were then immobilized by grafting onto SBA-15 silica following procedures previously reported elsewhere<sup>[72]</sup> and the resulting hybrid materials are denoted in this study as **Pd( $\text{PPh}_2$ )<sub>2</sub>/SBA-15**, **Pd( $\text{PCy}_2$ )<sub>2</sub>/SBA-15** and **Pd( $\text{PNP}$ )/SBA-15**, respectively (Figure 1, top). Additionally, in order to evaluate what effect the spatial location of Pd sites in the solid has on leaching, one of these Pd complexes bearing Alkyl- $\text{PPh}_2$  as ligand was encapsulated within the silica framework using a synthesis adapted from a procedure described by Dufaud et al. and which leads to SBA-3 mesostructured silicas.<sup>[73]</sup> Typically, siloxanes containing Pd complex,  $\text{PdCl}_2\{\text{PPh}_2[\text{CH}_2\text{CH}_2\text{Si}(\text{OR})_3]\}_2$ , was co-hydrolyzed and polycondensed with TEOS (tetraethyl orthosilicate) in the presence of CTAB (cetyltrimethylammonium bromide) used as structure directing agent (SDA) in a mixture of water, HCl and acetonitrile (see Experimental Section). The synthesis was carried out at low temperature (25 °C) and short reaction time (4 h) to preserve the integrity of the molecular precursor. The resulting solid was then silylated with  $\text{TMSCl}$  in toluene prior to SDA removal in order to maintain the mesostructuration of the material named as **Pd( $\text{PPh}_2$ )<sub>2</sub>@SBA-3** (Figure 1, bottom).

All solid materials were fully characterized using molecular and bulk analytical and spectroscopic techniques. The results obtained for the three grafted derived solids, **Pd( $\text{PPh}_2$ )<sub>2</sub>/SBA-15**, **Pd( $\text{PCy}_2$ )<sub>2</sub>/SBA-15** and **Pd( $\text{PNP}$ )/SBA-15**, were in full agreement with previously reported characterizations.<sup>[72]</sup> We have summarized in Table 1 only the main textural and physical characteristics for comparison with **Pd( $\text{PPh}_2$ )<sub>2</sub>@SBA-3**. The XRD pattern of the latter ex-

**Table 1.** Physical and textural properties of palladium containing hybrid silica materials.

Catalyst	Pd [%wt]	$d_{100}^{[a]}$ [Å]	$a_0^{[b]}$ [Å]	Wall thickness <sup>[c]</sup> [Å]	$V_p^{[d]}$ [cm <sup>3</sup> g <sup>-1</sup> ]	$D_p^{[e]}$ [Å]	$S_{BET}$ [m <sup>2</sup> g <sup>-1</sup> ]	$C_{BET}$
<b>Pd(PPh<sub>2</sub>)<sub>2</sub>@SBA-3</b>	0.31	35	41	18	0.58	23	1009	15
<b>Pd(PPh<sub>2</sub>)<sub>2</sub>/SBA-15</b>	3.06	96	111	56	0.66	54	601	181
<b>Pd(PCy<sub>2</sub>)<sub>2</sub>/SBA-15</b>	1.21	100	115	53	0.80	63	458	102

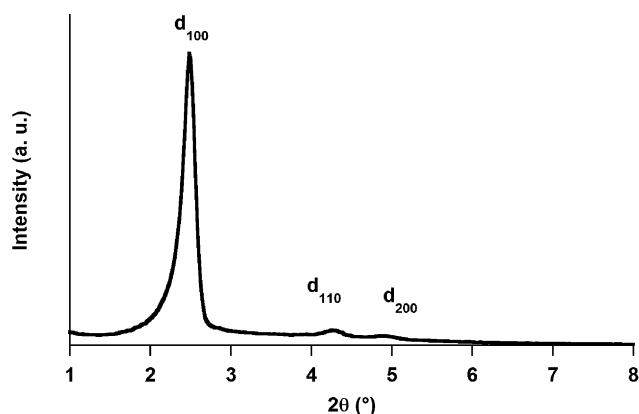
[a]  $d(100)$  spacing.

[b]  $a_0 = 2d(100)/\sqrt{3}$ , hexagonal lattice parameter calculated from XRD.

[c] Calculated by  $a_0$ -pore size.

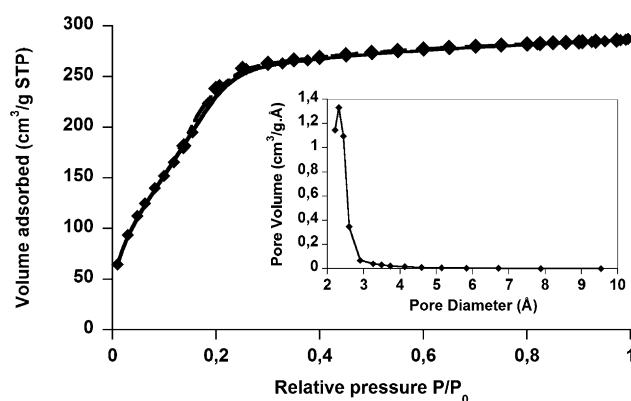
[d] Total pore volume at  $P/P_0 = 0.980$ .

[e] Pore size from desorption branch applying the BJH pore analysis except for **Pd(PPh<sub>2</sub>)<sub>2</sub>@SBA-3** where the adsorption branch was used.

**Figure 2.** XRD pattern of palladium containing SBA-3 silica embedded into the silica walls.

hibited three well-resolved peaks at  $2\theta$  values between 2–5° that can be indexed as (100), (110) and (200) diffractions which is typical for a well ordered 2D hexagonal mesostructure (Figure 2). The  $d(100)$  spacing was found to be *ca.* 36 Å which corresponds to a unit cell parameter of 41 Å. The presence of higher order reflections indicates that the preparation method allowed for the synthesis of a long-range structural ordered **Pd(PPh<sub>2</sub>)<sub>2</sub>@SBA-3** hybrid material. No strong modification in the unit cell parameters was observed between the hybrid (41 Å) compared to the parent SBA-3 (38 Å) attesting that the Pd complex is effectively inserted in the walls rather than in the pores.

Nitrogen adsorption-desorption measurement showed a type IV isotherm, characteristic of mesoporous solids, with a relatively smooth capillary condensation step appearing at relative pressure of  $P/P_0 = 0.3$  (Figure 3 left) which indicates the presence of regular pores in the sample. This was also confirmed by a narrow pore diameter distribution in the micro/mesopore range (Figure 3 right). High BET surface area (1009 m<sup>2</sup>g<sup>-1</sup>) was obtained with average pore diameters and pore volumes of respectively 23 Å and 0.58 cm<sup>3</sup>g<sup>-1</sup>. These values are close to those obtained for metal-free SBA-3 (i.e., respectively, 1024 m<sup>2</sup>g<sup>-1</sup>,

**Figure 3.** Nitrogen adsorption/desorption isotherm and pore size distribution (insert; from adsorption branch applying the BJH pore analysis) of **Pd(PPh<sub>2</sub>)<sub>2</sub>@SBA-3**.

< 20 Å and 0.50 cm<sup>3</sup>g<sup>-1</sup>, see Table S1 in the Supporting Information) in agreement with inclusion of the Pd complex inside the walls.

**Pd(PPh<sub>2</sub>)<sub>2</sub>@SBA-3** was found to contain 0.31 wt% Pd and 0.16 wt% P (P/Pd ~1.8) suggesting that the integrity of the molecular precursor PdCl<sub>2</sub>{PPh<sub>2</sub>[CH<sub>2</sub>CH<sub>2</sub>Si(OR)<sub>3</sub>]}<sub>2</sub> was maintained throughout the synthesis with on average two phosphorus atoms per palladium centre.

The <sup>29</sup>Si CP-MAS NMR spectrum (Supporting Information, Figure S1) displayed discernable peaks in two different spectral regions. One region ranging from -80 to -120 ppm characteristic of Q-type [Q<sup>n</sup> = Si-(OSi)<sub>n</sub>-(OH)<sub>4-n</sub>] silicates originating from the siliceous bulk material with Q<sup>2</sup>, Q<sup>3</sup> and Q<sup>4</sup> at, respectively, -89, -100 and -109 ppm. A single resonance at 14 ppm typical of M-type [R<sub>3</sub>Si(O-)] silicates was attributed to the trimethylsilyl capped silanol groups. T-type [T<sup>m</sup> = RSi(OSi)<sub>m</sub>-(OH)<sub>3-m</sub>] silicates, that is the silicon atoms attached to the phosphine through the alkyl chain, expected in the -40 to -70 ppm spectral region, were not discernable likely due to the low Pd and phosphorus contents in the solid.

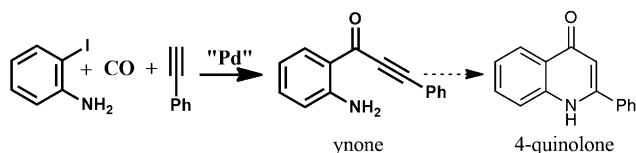
Solid-state MAS <sup>31</sup>P NMR spectroscopy proved to be a useful technique to elucidate the structural integ-

rity and coordination mode of the phosphine linkers at the palladium centre in  $\text{Pd}(\text{PPh}_2)_2\text{@SBA-3}$ . The  $^{31}\text{P}$  MAS NMR spectrum (Supporting Information, Figure S2) exhibits a relatively broad signal centred at 21 ppm attributed to the *trans*-isomer of the Pd precursor; however, one cannot exclude the presence of the corresponding *cis*-isomer ( $\delta=30$  ppm) for which the relative intensity should be rather low due to the low Pd loading. The Pd–P bond seemed unaffected: no signal corresponding to free phosphine ligands ( $\delta=9$  ppm) was detected.

Comparing the textural properties of  $\text{Pd}(\text{PPh}_2)_2\text{@SBA-3}$  to those of the other Pd catalysts prepared by simple grafting onto SBA-15 type silica (Table 1), we observed that this material is in the lower range of mesoporous solids, near to that of microporous materials; the structure appears to be more contracted with smaller pore sizes (23 Å *versus ca.* 54–63 Å) and thinner walls (18 Å *versus ca.* 53–63 Å) than those based on SBA-15 with however a higher specific surface area attributed to the inclusion of the Pd complex inside the walls rather than held at the surface of the pores. Moreover, the  $C_{\text{BET}}$  coefficient indicates a hydrophilic surface in the case of SBA-15 based materials with an average value of 131 and a hydrophobic surface for the  $\text{Pd}(\text{PPh}_2)_2\text{@SBA-3}$  hybrid ( $C_{\text{BET}}=15$ ) which is a direct consequence of the silylation of the remaining silanol groups on the surface of this latter material. These variations can affect the “boomerang effect” and can provide important information concerning deactivation processes.

### Evaluation of Catalytic Efficiency of the Different Materials

In the field of our studies related to the synthesis of 4-quinolones from 2-iodoanilines, terminal alkynes and carbon monoxide, we demonstrated that ynones were intermediately formed before cyclization to deliver the target compound (Scheme 1). In these studies, we also demonstrated that ynones were produced through a Pd-catalyzed cross-coupling, whereas cyclization occurred under amine catalysis.<sup>[24,25]</sup> Thus, decreasing the Pd leaching during the formation of the ynone intermediate should reduce the Pd contamination in the final target compound.



**Scheme 1.** Synthetic strategy for the formation of 4-quinolone: palladium-catalyzed carbonylative Sonogashira coupling and subsequent cyclization of the obtained ynone.

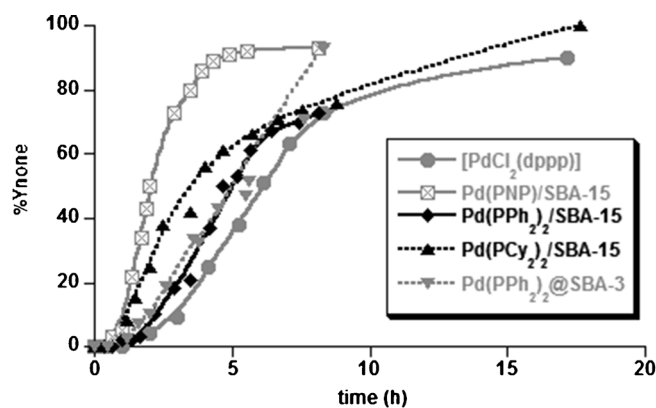


**Figure 4.** Kinetic curves for the different Pd hybrid materials and comparison to the homogeneous  $[\text{PdCl}_2(\text{dppp})]$ . Conditions: iodoaniline (6 mmol), phenylacetylene (1.2 equiv.),  $[\text{Pd}]$  (0.1 mol %), triethylamine (2.5 equiv.), anisole (10 mL), 5 bar CO, 80 °C.

All hybrid materials were evaluated for the synthesis of 1-(2-aminophenyl)-3-phenylprop-2-yn-1-one from 2-iodoaniline, phenylacetylene and carbon monoxide through kinetic experiments (Figure 4). A full selectivity toward the expected ynone was observed for all the catalytic materials. The results were compared to those issued from the reaction using the homogeneous  $[\text{PdCl}_2(\text{dppp})]$  complex, which was found to be very selective in this transformation according to our previous studies.<sup>[24]</sup>

All catalysts proved to be effective in this coupling giving generally high conversions and selectivities toward the expected ynone. The highest reaction rates ( $v_{\text{max}}$ ), as measured at the maximum of the slope, delivered values for the hybrid materials in the same range or higher than that obtained with the homogeneous complex (Table 2, entry 1). Among the evaluated hybrid materials,  $\text{Pd}(\text{PNP})/\text{SBA-15}$  showed the highest rate (1.2  $\text{mmol h}^{-1}$ ) that is 3 times higher than that of  $[\text{PdCl}_2(\text{dppp})]$  (0.4  $\text{mmol h}^{-1}$ ).

On the basis of these results, no clear influence of the structure of the support was observed  $\text{Pd}(\text{PPh}_2)_2\text{@SBA-3}$  and  $\text{Pd}(\text{PPh}_2)_2/\text{SBA-15}$  showing nearly the same tendency. Thus, the palladium contamination in the crude product was determined, in a first approach, for two of the hybrid materials, namely  $\text{Pd}(\text{PCy}_2)_2/\text{SBA-15}$  and  $\text{Pd}(\text{PNP})/\text{SBA-15}$  which exhibited the highest reaction rates (Figure 4). This determination measured by ICP-AES was found to be, respectively, 1.4 ppm and 10 ppm. In both cases, these values are lower than that achieved when using the homogeneous catalyst (47 ppm). As this Pd contamination finds generally its origin in the leaching of metal species from the solid catalysts during reaction, we undertook a systematic study of this leaching process using the well-known hot-filtration technique (see below) to determine whether the reaction occurs

**Table 2.** Reaction rates, activities and leaching ratios for the different Pd catalysts.

Catalyst		Entry 1 $v_{\max}$ [mmol h <sup>-1</sup> ]	Entry 2 Leaching ppm	Entry 3 %	Entry 4 $A_{\max}$ [mol/min mol <sup>-1</sup> <sub>Pd</sub> ]
Homogeneous	[PdCl <sub>2</sub> (dppp)]	0.4	47	100	2
In the pores	Pd(PCy <sub>2</sub> ) <sub>2</sub> /SBA-15	0.6	3	6	52
	Pd(PPh <sub>2</sub> ) <sub>2</sub> /SBA-15	0.5	4	7	37
	Pd(PNP)/SBA-15	1.2	22	47	15
In the walls	Pd(PPh <sub>2</sub> ) <sub>2</sub> @SBA-3	0.4	10	20	11

via a true heterogeneous process or through a dissolution-redeposition process.

### Hot-Filtration Test and Determination of Pd Content in Solution

Estimation of the leaching rate was performed by two complementary determinations. In a first set of experiments, hot-filtration tests were performed for all materials. Typically, a standard catalytic run was initially started and after 2–4 h of reaction, which corresponds to 15–30% conversion, the reaction mixture was filtered through a hot syringe filter (PTFE, 0.45 μm) to afford a clear filtrate. The clear filtrate was then treated as a standard catalytic run and its

evolution followed by GC. The results were compared to that of a standard catalytic run in the presence of the solid material. As shown in Figure 5, all hybrid materials exhibited a more or less pronounced leaching phenomenon. Comparing the kinetics obtained with or without the heterogeneous catalyst clearly indicates that the coupling reaction was mainly catalyzed by dissolved Pd species, the participation of heterogeneous palladium being minor.

Two trends were observed regardless of the nature of the support or that of the immobilized Pd-complex. For Pd(PCy<sub>2</sub>)<sub>2</sub>/SBA-15 and Pd(PPh<sub>2</sub>)<sub>2</sub>/SBA-15, an important decrease in the reaction rate was observed after the removal of the solid material, although further conversion is observed. Thus we cannot exclude the possibility of the contribution of the solid material

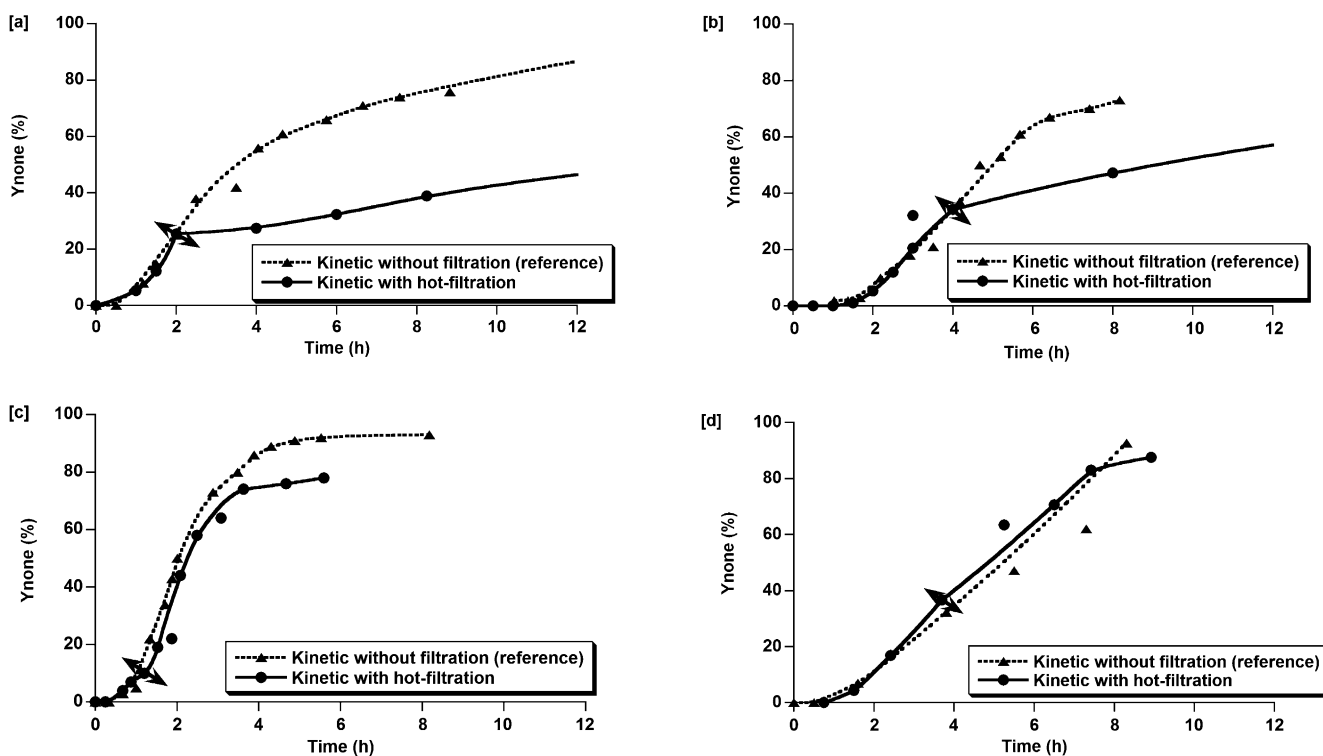


**Figure 5.** Comparison between hot filtration tests (solid line) and “standard” kinetic runs (dotted line) or [a] Pd(PCy<sub>2</sub>)<sub>2</sub>/SBA-15, [b] Pd(PPh<sub>2</sub>)<sub>2</sub>/SBA-15, [c] Pd(PNP)/SBA-15 and [d] Pd(PPh<sub>2</sub>)<sub>2</sub>@SBA-3. The hot-filtration is symbolized by the double-headed arrow.

to the catalytic reaction rate for these two materials, but this is very likely as a Pd reservoir rather than a true heterogeneous catalyst. For **Pd(PNP)/SBA-15** and **Pd(PPh<sub>2</sub>)<sub>2</sub>@SBA-3**, the situation was quite different since no significant changes in the reaction rates were observed after removal of the solid material which suggests that the reaction proceeds only through dissolved species.

In order to gain a deeper understanding in those two different behaviours, we measured the (dissolved) palladium content in the clear filtrates by ICP-AES (Table 2, entry 2). The leaching ratio was then calculated referring to the initial palladium loading at the beginning of the reaction run (Table 2, entry 3).

It clearly appears that the two materials for which the hot filtration has an important impact on the reaction rate are those for which the leaching ratio is the lowest, namely **Pd(PPh<sub>2</sub>)<sub>2</sub>/SBA-15** and **Pd(PCy<sub>2</sub>)<sub>2</sub>/SBA-15** with, respectively, 7% and 6%. This correlates with the proposed role of the solid material as a Pd reservoir, the leached species having a tendency to deactivate with time. Note that this deactivation phenomenon is not counterbalanced either by a high Pd concentration, or by a continuous dissolution of active Pd species in solution or a stabilization of the soluble species through the ligand or the support as would be the case in homogeneous catalysis or when heterogeneous solid is present. This situation contrasts severely with **Pd(PPh<sub>2</sub>)<sub>2</sub>@SBA-3** and **Pd(PNP)/SBA-15** for which significant amounts of leached Pd species were measured (10 ppm and 22 ppm, respectively). Thus, whatever the deactivation process of these dissolved Pd species, the deactivation will have dramatic effects in the former cases due to the low Pd concentration in solution whereas it is somewhat counterbalanced for the latter regarding the higher leaching ratio.

From those leached palladium amounts, activities can also be estimated by dividing the maximum reaction rate by the concentration of dissolved palladium (Table 2, entry 4). As expected from a direct consequence of the low leaching ratios, **Pd(PPh<sub>2</sub>)<sub>2</sub>/SBA-15** and **Pd(PCy<sub>2</sub>)<sub>2</sub>/SBA-15** showed the best activities, with 37 mol/min mol<sup>-1</sup><sub>Pd</sub> and 52 mol/min mol<sup>-1</sup><sub>Pd</sub>, respectively, the poorer activity (2 mol/min mol<sup>-1</sup><sub>Pd</sub>) being that of the homogeneous catalyst [PdCl<sub>2</sub>(dppp)]. Figure 6 illustrates the dependence between the measured Pd content in solution and the resulting determined catalyst activity (that is closely related to dissolved palladium) which correlates well with the postulate of De Vries based on the use of homeopathic Pd loading<sup>[74,75]</sup> and a deactivation process through aggregation of dissolved Pd species resulting in the formation of inactive palladium particles.<sup>[76,77]</sup> Thus, the highest Pd concentration in solution did not result in the highest measured catalyst activity.

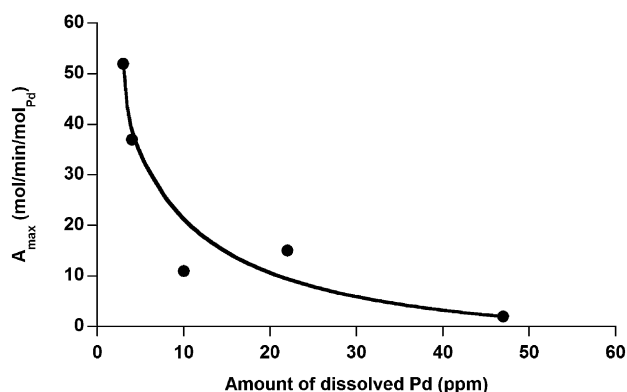


Figure 6. Correlation between lixiviation and activity.

### Parameters Influencing Pd Leaching from Pd(PNP)/SBA-15

In order to identify parameters influencing this leaching phenomenon a study was undertaken using **Pd(PNP)/SBA-15** as this hybrid material showed the highest leaching ratio (47%) in reaction among those evaluated. The catalyst was suspended in solvent under an Ar or CO atmosphere and heated at 80°C for 1 h. The suspension was then “hot-filtered” at 80°C. In a parallel experiment, the suspension was cooled to room temperature prior to filtration. The palladium amounts in the filtrates were measured by ICP-AES. From the hot-filtration tests the leaching ratio can be determined referring to the initial amount of Pd introduced. From the cooled-filtration tests, determination of palladium in solution allows one to calculate the redeposition ratio by comparing the Pd concentrations in “hot” and “cooled” solutions.

The results reported in Table 3 indicate, firstly, that the leaching ratio is not strongly influenced by the presence of reagents (Table 3, entries 1 and 2). Thus, the oxidative addition is not the triggering factor of the leaching phenomenon as dissolution of palladium occurred without reactants. This result is to be expected when using catalysts based on immobilized molecular complexes as the initial “activation” step is most probably the molecular transformation of the Pd complex to allow oxidative addition (according to the generally accepted mechanism using homogenous soluble Pd species in cross-coupling reactions); that contrasts with situations in which heterogeneous catalysts bearing immobilized palladium particles are used.

The role of working atmosphere is not so trivial. Apparently, working under CO or an inert atmosphere of Ar did not influence the leaching ratio (Table 3, entry 2 vs. 3) despite the ability of carbon monoxide to coordinate Pd species, thus, providing a stabilization of leached species in solution. Our results are in accordance with those reported by Davies

**Table 3.** Influence of different parameters on leaching and redeposition for **Pd(PNP)/SBA-15**.<sup>[a]</sup>

Entry	Atmosphere	Solvent	Silica	[Pd] in hot solution [ppm]	Leaching ratio [%] <sup>[b]</sup>	[Pd] in cooled solution [ppm]	Redeposition ratio [%] <sup>[c]</sup>
1 <sup>[d]</sup>	CO (5 bar)	anisole/NEt <sub>3</sub>	–	22	47	10	54
2	CO (5 bar)	anisole	–	29	48	13	55
3 <sup>[e]</sup>	Ar (PA)	anisole	–	28	47	24	14
4	Ar (PA)	toluene	–	2	3	2	0
5	Ar (PA)	anisole/NEt <sub>3</sub> <sup>[f]</sup>	–	25	42	25	0
6	Ar (PA)	anisole	silylated <sup>[g]</sup>	8	13	8	0
7	Ar (PA)	anisole <sup>[h]</sup>	–	12	20	8	33
8	Ar (PA)	NMP	–	34	57	34	0
9	Ar (PA)	DMF	–	38	64	38	0
10 <sup>[i]</sup>	Ar (PA)	DMF:H <sub>2</sub> O 1:1 <sup>[i]</sup>	–	29	48	17	41
11	Ar (PA)	NEt <sub>3</sub>	–	22	37	20	9

<sup>[a]</sup> Conditions: 8 mg **Pd(PNP)/SBA-15** ( $3.10^{-3}$  mmol Pd), solvent 5 mL, 80 °C, 1 h.

<sup>[b]</sup> Referring to the initial amount of palladium introduced.

<sup>[c]</sup> Represents redeposition of leached Pd.

<sup>[d]</sup> Values issued from Table 2 obtained in reaction (i.e., in presence of the reactants).

<sup>[e]</sup> The <sup>31</sup>P NMR spectroscopy was performed on the material after experiment.

<sup>[f]</sup> In the proportions used in reaction: 5 mL of anisole and 1.1 mL of NEt<sub>3</sub>.

<sup>[g]</sup> Preparation described in the Supporting Information.

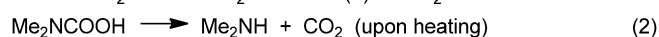
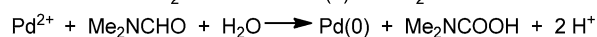
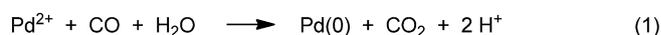
<sup>[h]</sup> 92 mg of “blank” SBA-15 silica was added.

<sup>[i]</sup> A hydrophilic filter was used (Millipore® HVLP type, 0.45 μm).

et al. who demonstrated through a three-phase test that carbon monoxide was not required to initiate the leaching of Pd to generate active species in palladium-catalyzed carbonylative coupling.<sup>[32]</sup> However, the atmosphere plays a role in the redeposition process (see discussion below).

By contrast, the hydrophilic/hydrophobic nature of the surface of the solid catalyst proved to have a significant influence on the stability of supported Pd species against leaching. Indeed, when the surface of the material was silylated with a hydrophobic trimethylsilyl group (see the Supporting Information for this procedure), the leaching ratio could be decreased from 47% to 13% (Table 3, entry 6 vs. 3). Such an observation has been previously reported for a copper catalyst grafted on SBA-15 silica and used in epoxidation reactions,<sup>[78]</sup> or Ti-MCM-41 catalyst applied in oxidative desulfurization<sup>[79]</sup> and epoxidation.<sup>[80]</sup> Unfortunately, from these results, it seems that the surface hydrophobization also prevents redeposition of leached species as was already observed in some polymeric materials bearing Pd complexes and used in cross-coupling reactions.<sup>[81,82]</sup> These results are in agreement with what was observed during the catalytic run while using **Pd(PPh<sub>3</sub>)<sub>2</sub>@SBA-3** catalyst whose surface had been silylated with TMSCl prior to surfactant removal (Table 2) when considering the longer reaction time for the latter and the reduced redeposition capacity. All together, these results suggest that such hydrophobic hybrid materials would act as Pd reservoirs but with probably lower recycling capacity due to the very limited redeposition process.

As often demonstrated in the literature, the solvent also may drastically influence the degree of leaching, less polar solvents leading, in general, to strongly decreased leaching ratio while polar solvents seem to favour metal extraction from the solid. Thus, except for the case where the surface of the catalyst was passivated, all polar solvents (i.e., anisole, DMF, DMF/H<sub>2</sub>O, NMP, NEt<sub>3</sub>) afford important palladium dissolution in the bulk solution, an observation in full agreement with almost all reports concerning Pd-catalyzed cross-coupling reactions that are generally carried out in such media. These conclusions are strongly supported by the results observed when using a less polar solvent such as toluene in which only a leaching ratio of 3% (vs. 40–65%) is observed (Table 3, entry 3). This tendency can find an explanation by the possible stabilization of small Pd-clusters in solution when using polar solvents, like anisole or triethylamine.<sup>[83]</sup> If the solvent plays apparently a role on the leaching ratio, it also plays a role on the redeposition. Thus, higher redeposition (41%) is observed when using the mixture DMF/H<sub>2</sub>O. This result can be compared with that observed under CO atmosphere (55% redeposition). In both cases reducing conditions are achieved either due to CO as reducing agent of Pd(II) species, or to the DMF/H<sub>2</sub>O mixture that was previously described to have reducing properties of metallic species, according to the following Eqs. (1) and (2):



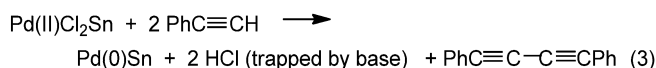
The difference observed between DMF (no redeposition) and DMF/H<sub>2</sub>O mixture (41% redeposition) lies to the fact that reducing conditions are only achieved in the presence of water (Table 3, entry 10 vs. 9). According to Köhler's reports,<sup>[42,59]</sup> reducing conditions help considerably to recover the dissolved palladium species by precipitation/stabilization at the solid surface.

An interesting way to reduce the leaching ratio was found by adding to the Pd catalyst additional blank SBA-15. Thus, working with a mixture of **Pd(PNP)/SBA-15** and **SBA-15** (1:10) allowed us to reduce the overall leaching ratio by a factor 2.4, that is closely related to the higher redeposition process (33% vs. 14%) provided by the higher availability of silica surface (Table 3, entry 7 vs. 3). The corollary of this observation is that a decrease in the Pd loading in the hybrid material will probably result in a higher redeposition possibility, hence reducing the overall leaching ratio.

While the leaching of palladium in solution from supported Pd particles is generally related to the initial oxidative addition of reagents, that from immobilized molecular Pd complexes can have several origins: the cleavage of the link between the surface and the complex, the pure loss of palladium through decoordination or the degradation of the ligand leading to the loss of some palladium. In order to answer this question, we examined both the solution and the solid catalyst after a standard catalytic run using <sup>31</sup>P NMR spectroscopy. No phosphorus signal was detected in the <sup>31</sup>P NMR spectrum of the solution thus ruling out any phosphine degradation (at the silicon or at the organic spacer) and subsequent extraction. This conclusion was further supported by solid state <sup>31</sup>P NMR of the material (Supporting Information, Figure S3) that showed a broad signal corresponding to the Pd-coordinated phosphine (+10 ppm). No signals related to free phosphine (−28 ppm) could be detected on <sup>31</sup>P NMR; however, we cannot fully exclude the formation of phosphine oxide (+28 ppm) following the loss of coordinated palladium that could be expected regarding the leaching ratio and the relatively low Pd redeposition. Thus, from these analyses we can conclude that the main route toward leaching under our reaction conditions is related to the decoordination of Pd from the original immobilized complex.

In summary, we have demonstrated in this study that the leaching of palladium from hybrid material bearing immobilized Pd complexes could be caused by other phenomenon than the oxidative addition since neither carbon monoxide nor the base or the reagents were required to initiate the solubilization of the metal. Palladium decoordination from the grafted complexes, very probably triggered by temperature and favoured by the stabilizing nature of polar solvent, is more likely responsible for the metal leaching.

Palladium would thus be leached as Pd(II) species as PdCl<sub>2</sub>S<sub>n</sub> before being reduced in solution to give a Pd(0)S<sub>n</sub> species that enters in the catalytic cycle. Reduction can be done by CO combined with traces of water [see Eq. (1)] or by the formation of alkyne dimers [Eq. (3)]:



Some directions aiming at reducing the overall leaching point out the control of the surface philicity to reduce leaching as well as the reduction of Pd loading in order to maximize available silica surface for the redeposition process, the latter being favoured under reducing conditions.

### Characterization of the Catalysts after Reaction

While we demonstrated that the presence of reactants was not necessary to initiate leaching of Pd species in solution, we were, however, interested to investigate how it can influence leaching and redeposition rates and to some extent recycling efficiency. Therefore, various analyses [i.e.: elemental analysis (P, Pd), small- and wide-angle XRD and MAS <sup>31</sup>P NMR] were performed on the catalytic solids after a single run and are displayed in the Supporting Information. Three catalysts were evaluated, namely **Pd(PNP)/SBA-15**, **Pd(PCy<sub>2</sub>)<sub>2</sub>/SBA-15** and **Pd(Ph<sub>2</sub>)<sub>2</sub>@SBA-3**.

For all catalysts, small angle XRD patterns (Supporting Information, Figures S6, S10 and S13) showed long-range mesoscopic ordering, indicating that the mesostructure remained intact during the course of the reaction. However, depending on the catalysts, other analyses showed differences.

For **Pd(PCy<sub>2</sub>)<sub>2</sub>/SBA-15**, the P/Pd ratio determined by elemental analysis on the fresh and the used catalyst (Supporting Information, Table S3) did not change significantly after reaction. This result is in accordance with the low leaching ratio observed for this catalyst (6%, Table 2). MAS <sup>31</sup>P NMR (Supporting Information, Figure S9 vs. S8) showed, however, two broad signals that could be attributed to initially complexed phosphine and phosphine oxide. Thus, considering that palladium is not coordinated to phosphine oxide, we can determine a leaching ratio from <sup>31</sup>P NMR of 11% which is close to that calculated from the hot-filtration experiment. These results point out that elemental analysis alone cannot be used to rule out a possible leaching of the metal during reaction, particularly when the leaching rate is low, due to the precision limits of this analysis. The presence of phosphine oxide, in combination with the stable P/Pd ratio, could indicate that palladium could be redepos-

ited on the support, probably as very small Pd particles, since no signal attested the formation of Pd particles in wide angle XRD (Supporting Information, Figure S11).

For **Pd(PPh<sub>2</sub>)<sub>2</sub>@SBA-3**, an increase of the P/Pd ratio (Supporting Information, Table S4) was observed after reaction indicating a loss of Pd of *ca.* 30% which is in agreement with the leaching ratio measured during reaction (20%, Table 2). For this catalyst, due to the low Pd complex loading, the intensity of the signals obtained in MAS <sup>31</sup>P NMR were too low to determine the existence of leaching in the presence of de-coordinated or oxidized phosphines.

**Pd(PNP)/SBA-15** showed a very different behaviour in the presence of reagents (i.e., iodoaniline, phenylacetylene) compared to what was observed in leaching/redeposition experiments realized in sole solvent (Table 3). While we demonstrated through <sup>31</sup>P MAS NMR that the phosphine ligand was stable in the absence of reagents, the <sup>31</sup>P NMR of the material performed after a reaction run clearly indicates a degradation of the ligand with a single broad signal centered at -4 ppm that could not be attributed to Pd-coordinated phosphine (expected at +7–11 ppm), phosphine oxide (*ibid* +28 ppm) or free phosphine (*ibid* -28 ppm). Additionally, the decrease of the P/Pd ratio (Supporting Information, Table S2) indicates a loss of phosphorus that is connected to a relatively good Pd-redeposition (54%, Table 3, entry 1) as attested by wide angle XRD performed on the material after reaction that showed a small peak at 2θ = 40° attributed to metallic Pd particles (Supporting Information, Figure S7). This confirms the role played by CO: given that a high leaching ratio is observed, Pd redeposits on the non-silylated support as *large* particles, a phenomenon which is favoured by the reducing CO atmosphere. To date, the best explanation for the lack of stability of the (PNP)-ligand under the reaction conditions lies in the basic conditions used to perform the catalytic run leading to degradation of the (PCH<sub>2</sub>NCH<sub>2</sub>P) linkages once the Pd atom is de-coordinated.

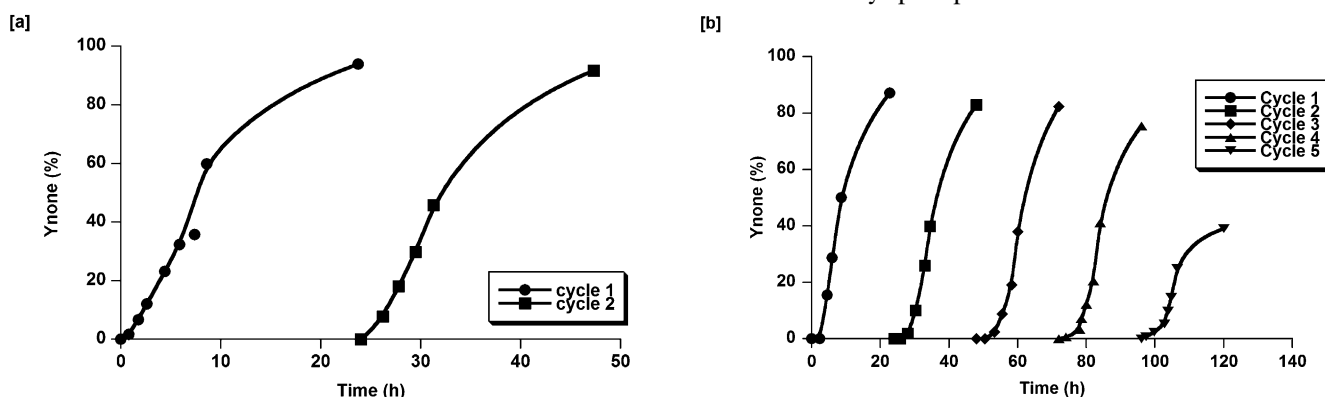


**Figure 7.** Kinetic curves of the different runs for the recycling of [a] **Pd(PNP)/SBA-15** and [b] **Pd(PPh<sub>2</sub>)<sub>2</sub>/SBA-15** in the presence of an added amount of “blank” SBA-15.

The above results are in accordance with a Pd redeposition as small particles on the silica surface stabilized by remaining silanol groups, an effect favoured by the high specific area of the SBA-15 silicas.

## Recycling

Even though heterogeneous catalysts are generally not reused in industrial pharmaceutical syntheses because of the risk of cross contaminations, we decided to perform recycling studies with two of the evaluated hybrid materials, namely, **Pd(PNP)/SBA-15** and **Pd(PPh<sub>2</sub>)<sub>2</sub>/SBA-15**, which differ by their leaching extents, respectively, of 47% and 7%. Figure 7 clearly evidences that both materials could be reused without any regeneration or reactivation. Unfortunately, experimental difficulties in recovering the **Pd(PNP)/SBA-15** material prevented further evaluation. On the other hand, **Pd(PPh<sub>2</sub>)<sub>2</sub>/SBA-15** could be reused up to four times without noticeable deactivation which was only observed during the fifth run with a drop in the  $V_{\max}$  to 0.32 mmol h<sup>-1</sup> leading to a limited conversion of 39% in 24 h (Table 4). For this catalyst, a TON of over 6000 was determined demonstrating its high efficiency. The loss of activity observed upon recycling can be due to limitations in the Pd redeposition as observed in our tests and/or mass loss of catalytic material upon such successive recovery series.

## Preparation of Other Yrones

This optimized methodology was then applied to the synthesis of several yrones. In all reactions, the selectivity reached using heterogeneous catalysts was higher than that observed with homogeneous catalytic systems<sup>[24]</sup> as full selectivity toward the expected ynone was achieved. Indeed, on the contrary to the previously described homogeneously catalyzed reactions, no cyclization of the yrones towards indoxyl – as activated by phosphines – was observed. As is

**Table 4.** Maximum reaction rates along the successive runs for the recycling of **Pd(PNP)/SBA-15** and **Pd(PPh<sub>2</sub>)<sub>2</sub>/SBA-15**.

Catalyst	Cycle	$v_{\max}$ [mmol h <sup>-1</sup> ]	Conv. at 24 h [%]
<b>Pd(PNP)/SBA-15</b>	1	0.57	94
	2	0.45	92
<b>Pd(PPh<sub>2</sub>)<sub>2</sub>/SBA-15</b>	1	0.53	87
	2	0.48	83
	3	0.53	82
	4	0.53	75
	5	0.32	39

likely in homogeneous systems, no product resulting from simple Sonogashira coupling (i.e., non-carbonylated product) was detected. Thus, using **Pd(PNP)/SBA-15** as catalyst various ynones were obtained with isolated yields ranging from 58% to 81% (Table 5, see Supporting Information for more details).

## Conclusions

The synthesis of propynone by heterogeneously palladium-catalyzed carbonylative Sonogashira coupling was studied, focusing on the behaviour of the catalytic materials in reaction especially toward “boomerang” (i.e., leaching/redeposition) phenomena. Several organophosphino-palladium complexes grafted on SBA-15 silica or incorporated within the walls of SBA-3 silica were evaluated. The main results of these studies are: (i) the cross-coupling reaction of 2-iodoaniline with phenylacetylene under a CO atmosphere leading to the formation of ynones is catalysed by soluble spe-

cies, agreeing with literature reports; (ii) all the materials evaluated undergo Pd leaching at a more or less important level; (iii) when engaging immobilized Pd complexes, the leaching of Pd is not initiated through an oxidative addition step but rather by Pd decoordination from ligand probably favoured by temperature and solvent polarity.

The detailed study of the boomerang effect allowed us to identify some of the parameters that enable a decrease of the leaching (also through a better redeposition): (i) low grafting ratio; (ii) hydrophobic state of the surface; (iii) low polarity of the solvent; (iv) reducing conditions (either through the atmosphere or the solvent).

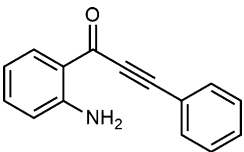
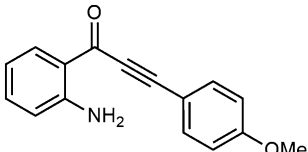
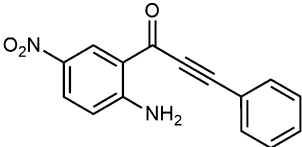
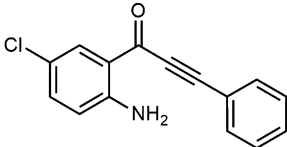
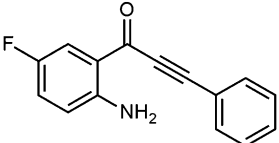
Despite leaching of metallic species from the support, the use of heterogeneous catalysts still remains interesting regarding the metal contamination issue of the final compounds compared to homogeneous catalysts since the contamination in the crude product was found in the best cases to be very close to the recommendation level of 10 ppm for oral intake of the European Agency for the Evaluation of Medicinal Products. As a result, several ynones were prepared thanks to this heterogeneous catalytic system achieving full selectivity toward desired compounds.

## Experimental Section

### Synthesis of Heterogeneous Pd Catalysts

**Pd(PPh<sub>2</sub>)<sub>2</sub>/SBA-15**, **Pd(PNP)/SBA-15** and **Pd(PCy<sub>2</sub>)<sub>2</sub>/SBA-15** were prepared by post-synthesis grafting of the corresponding molecular precursors onto SBA-15 silica as described elsewhere<sup>[72]</sup>.

**Table 5.** Synthesis of ynones.<sup>[a]</sup>

Product	Yield	Product	Yield
	64%		81%
	75%		70%
	58%		

<sup>[a]</sup> Conditions: 2-iodoaniline (3 mmol), alkyne (1.2 equiv.), **Pd(PNP)/SBA-15** (0.1 mol%), NEt<sub>3</sub> (2.5 equiv.), anisole, (5 mL), CO (20 bar), 80 °C, 10 h.

### Preparation of Pd(PPh<sub>3</sub>)<sub>2</sub>@SBA-3

This hybrid material was obtained in a three-step reaction sequence. Typically, CTAB (4.65 g) was suspended in water (118 g) and solubilized by addition of concentrated HCl (58 mL, 37% HCl). A portion of acetonitrile (6.6 g) was added and the solution was stirred for 15–30 min. TEOS (15.62 g) was then added dropwise (over 10 min). The supernatant of a suspension of PdCl<sub>2</sub>[PPh<sub>2</sub>(CH<sub>2</sub>)<sub>3</sub>Si(OEt)<sub>3</sub>]<sub>2</sub> (349 mg) in acetonitrile (6.6 g) was then slowly added to the gel which was then stirred at room temperature for 4 h and filtered on sintered glass. The solid was washed with HCl (1 M) then with water and dried under air overnight then under vacuum at 60 °C for 2 days. The material was then stabilized by silylation as follows: the material was suspended in toluene and TMSCl (21 mL) was added. The suspension was heated at 50 °C for 3 h then filtered, washed thoroughly with toluene and dried under vacuum overnight. The surfactant was then removed by extraction with warm ethanol (1 h at 50 °C, 3 successive extractions) and the material was dried under vacuum at 60 °C overnight. The molecular state of the resulting hybrid material was characterized by multi-nuclear NMR spectroscopy (<sup>31</sup>P and <sup>29</sup>Si NMR). The quantitative determination was assessed by elemental and thermogravimetric analyses and the textural and physical properties by nitrogen sorption measurements and powder X-ray diffraction at small angles (see Table S1 in Supporting Information for comparison with parent SBA-3 silica). <sup>29</sup>Si CP-MAS NMR: δ = 14, -89.5, -100, -109; <sup>31</sup>P MAS NMR: δ = 21; ICP-AES analysis: 0.31 wt % Pd, 0.16 wt % P.

### Catalytic Tests

**Kinetic experiments:** A mixture of 2-iodoaniline (6 mmol), alkyne (1.2 equiv.), [Pd] (0.1 mol%) and triethylamine (2.5 equiv.) in solvent (10 mL) was placed in a stainless autoclave which was purged twice at 20 bar with Ar and once with CO. The autoclave was charged with 5 bar CO and the mixture was stirred at 80 °C. For kinetic follow-up, the conversion was measured by regular GC sampling referring to an external standard (biphenyl) calibrated to the corresponding pure compound (experimental error ±5%). To obtain pure ynone, after completion of the reaction, the autoclave was depressurized and purged twice at 20 bar with Ar. The reaction medium was taken up with CH<sub>2</sub>Cl<sub>2</sub> (20 mL) and filtered on sintered glass. The filtrate was washed with NaHCO<sub>3</sub> (2 × 20 mL) then with brine (1 × 20 mL). The organic layer was dried over MgSO<sub>4</sub> and evaporated under reduced pressure. The residue was purified by chromatography on silica gel. See Supporting Information for details.

**Hot-filtration experiments:** The reaction was started as described above and the conversion was followed by GC sampling. At around 20–40% conversion, the autoclave was depressurized and opened by a small aperture on the lid. Immediately afterwards, the reaction medium was rapidly filtered off through a syringe filter (PTFE, 0.45 μm) preheated with warm solvent. The filtrate was then directly introduced in a second autoclave containing 1 equivalent of fresh triethylamine. This autoclave was then purged once with 20 bar CO, charged with 5 bar CO and heated at 80 °C. The evolution of the conversion in the filtrate was followed as before by GC sampling.

**Leaching and redeposition experiments:** Pd(PNP)/SBA-15 was suspended in a solvent under an Ar or CO atmosphere and heated at 80 °C for 1 hour. The suspension was then “hot filtrated” through a syringe PTFE, 0.45 μm filter or a hydrophilic Millipore® HVLP type, 0.45 μm filter (in the case of the DMF/H<sub>2</sub>O mixture) preheated with warm solvent. The palladium content in the filtrate was measured by ICP-AES. The leaching ratio was determined by comparison of the Pd amount in the hot filtrate and the initial Pd amount introduced in the material.

In parallel experiments, the suspension was first cooled down to room temperature and then filtrated. The palladium content in solution was also measured by ICP-AES. The redeposition ratio was calculated by comparison with the leaching ratio.

**Recycling experiments:** For these experiments, prior to its use, the catalyst was “diluted” by addition of an amount of non-functionalized SBA-15 silica (877 m<sup>2</sup>g<sup>-1</sup>) in order to reach a weight of 100 mg of material in the reaction mixture facilitating its separation. This was done with the aim of having a sufficient amount of material to isolate the solid by filtration after each run. Thus, after a first catalytic cycle, the mixture of catalyst and “blank” SBA-15 silica was separated by filtration, washed with DCM, MeOH and Et<sub>2</sub>O and dried under vacuum. It was then reused in the next cycle without further reactivation steps. The same stoichiometry as during the first cycle was used but the amounts of reactants and solvent were adjusted according to the collected amount of recovered solid.

### Acknowledgements

The authors gratefully acknowledge the National Agency of Research (No. ANR-07-BLAN-0167-01/02) for funding. M.G. thanks ANR for a fellowship. CNRS and Université Claude Bernard de Lyon 1 are kindly thanked for financial support. The authors kindly acknowledge the scientific services of IRCELYON for analyses and helpful discussions (C. Lorentz for Solid-Sate NMR, F. Bosselet and G. Bergeret for XRD, P. Mascunan and N. Cristin for ICP-AES analyses). The authors warmly thank G. Niccolai for proof reading our manuscript.

### References

- [1] C. A. Quesnelle, P. Gill, M. Dodier, D. St. Laurent, M. Serrano-Wu, A. Marinier, A. Martel, C. E. Mazzucco, T. M. Stickle, J. F. Barrett, D. M. Vyas, B. N. Balasubramanian, *Bioorg. Med. Chem. Lett.* **2003**, *13*, 519–524.
- [2] J. Marco-Contelles, E. de Opazo, *J. Org. Chem.* **2002**, *67*, 3705–3717.
- [3] C. J. Forsyth, J. Xu, S. T. Nguyen, I. A. Samdal, L. R. Briggs, T. Rundberget, M. Sandvik, C. O. Miles, *J. Am. Chem. Soc.* **2006**, *128*, 15114–15116.
- [4] A. Arcadi, M. Aschi, F. Marinelli, M. Verdecchia, *Tetrahedron* **2008**, *64*, 5354–5361.
- [5] H. Sheng, S. Lin, Y. Huang, *Tetrahedron Lett.* **1986**, *27*, 4893–4894.

- [6] A. Jeevanandam, K. Narkunan, C. Cartwright, Y.-C. Ling, *Tetrahedron Lett.* **1999**, *40*, 4841–4844.
- [7] A. V. Kel'i, V. Gevorgyan, *J. Org. Chem.* **2002**, *67*, 95–98.
- [8] P. Bannwarth, A. Valleix, D. Grée, R. Grée, *J. Org. Chem.* **2009**, *74*, 4646–4649.
- [9] T. Kobayashi, M. Tanaka, *J. Chem. Soc. Chem. Commun.* **1981**, 333–334.
- [10] T. Fukuyama, R. Yamaura, I. Ryu, *Can. J. Chem.* **2005**, *83*, 711–715.
- [11] T. Fukuyama, T. Rahman, M. Sato, I. Ryu, *Synlett* **2008**, 151–163.
- [12] B. Liang, M. Huang, Z. You, Z. Xiong, K. Lu, R. Fathi, J. Chen, Z. Yang, *J. Org. Chem.* **2005**, *70*, 6097–6100.
- [13] C. L. Li, X. L. Li, Q. Q. Zhu, H. Y. Cheng, Q. R. Lv, B. H. Chen, *Catal. Lett.* **2009**, *127*, 152–157.
- [14] W. B. Ma, X. L. Li, J. M. Yang, Z. L. Liu, B. H. Chen, X. F. Pan, *Synthesis* **2006**, 2489–2492.
- [15] M. S. Mohamed Ahmed, A. Mori, *Org. Lett.* **2003**, *5*, 3057–3060.
- [16] E. Awuah, A. Capretta, *Org. Lett.* **2009**, *11*, 3210–3213.
- [17] M. T. Rahman, T. Fukuyama, N. Kamata, M. Sato, I. Ryu, *Chem. Commun.* **2006**, 2236–2238.
- [18] P. J. Tambade, Y. P. Patil, N. S. Nandurkar, B. M. Bhanage, *Synlett* **2008**, 886–888.
- [19] C. Fehér, Á. Kuik, L. Márk, L. Kollár, R. Skoda-Földes, *J. Organomet. Chem.* **2009**, *694*, 4036–4041.
- [20] V. Sans, A. M. Trzeciak, S. Luis, J. J. Ziolkowski, *Catal. Lett.* **2006**, *109*, 37–41.
- [21] J. Liu, J. Chen, C. Xia, *J. Catal.* **2008**, *253*, 50–56.
- [22] Y. Liang, S. Liu, Y. Xia, Y. Li, Z.-X. Yu, *Chem. Eur. J.* **2008**, *14*, 4361–4373.
- [23] W. Hao, J. Sha, S. Sheng, M. Cai, *J. Mol. Catal. A: Chem.* **2009**, *298*, 94–98.
- [24] M. Genelot, A. Bendjeriou, V. Dufaud, L. Djakovitch, *Appl. Catal. A: Gen.* **2009**, *369*, 125–132.
- [25] M. Genelot, V. Dufaud, L. Djakovitch, *Tetrahedron* **2011**, *67*, 976–981.
- [26] N. Batail, M. Genelot, V. Dufaud, L. Joucla, L. Djakovitch, *Catal. Today* **2011**, *173*, 2–14.
- [27] L. Djakovitch, N. Batail, M. Genelot, *Molecules* **2011**, *16*, 5241–5267.
- [28] European Medicines Agency, *Guideline on the specification limits for residues of metal catalysts or metal reagents*, **2008**.
- [29] L. Djakovitch, P. Rollet, *Tetrahedron Lett.* **2004**, *45*, 1367–1370.
- [30] L. Djakovitch, P. Rollet, *Adv. Synth. Catal.* **2004**, *346*, 1782–1792.
- [31] L. Djakovitch, V. Dufaud, R. Zaidi, *Adv. Synth. Catal.* **2006**, *348*, 715–724.
- [32] I. W. Davies, L. Matty, D. L. Hughes, P. J. Reider, *J. Am. Chem. Soc.* **2001**, *123*, 10139–10140.
- [33] R. B. Bedford, C. S. J. Cazin, M. B. Hursthouse, M. E. Light, K. J. Pike, S. Wimperis, *J. Organomet. Chem.* **2001**, *633*, 173–181.
- [34] W. C. Shieh, R. Shekhar, T. Blacklock, A. Tedesco, *Synth. Commun.* **2002**, *32*, 1059–1067.
- [35] C. Baleizão, A. Corma, H. Garcia, A. Leyva, *J. Org. Chem.* **2004**, *69*, 439–446.
- [36] B. Blanco, A. Mehdi, M. Moreno-Manas, R. Pleixats, C. Rey, *Tetrahedron Lett.* **2004**, *45*, 8789–8791.
- [37] K.-i. Shimizu, S. Koizumi, T. Hatamachi, H. Yoshida, S. Komai, T. Kodama, Y. Kitayama, *J. Catal.* **2004**, *228*, 141–151.
- [38] O. Vassilyev, J. Chen, A. P. Panarello, J. G. Khinast, *Tetrahedron Lett.* **2005**, *46*, 6865–6869.
- [39] C. M. Crudden, M. Sateesh, R. Lewis, *J. Am. Chem. Soc.* **2005**, *127*, 10045–10050.
- [40] J.-S. Chen, A. N. Vasiliev, A. P. Panarello, J. G. Khinast, *Appl. Catal. A: Gen.* **2007**, *325*, 76.
- [41] J. M. Richardson, C. W. Jones, *J. Catal.* **2007**, *251*, 80–93.
- [42] K. Köhler, R. Heidenreich, S. Soomro, S. Pröckl, *Adv. Synth. Catal.* **2008**, *350*, 2930–2936.
- [43] L. Joucla, G. Cusati, C. Pinel, L. Djakovitch, *Tetrahedron Lett.* **2008**, *49*, 4738–4741.
- [44] J. A. Sullivan, K. A. Flanagan, H. Hain, *Catal. Today* **2009**, *145*, 108–113.
- [45] L. Joucla, G. Cusati, C. Pinel, L. Djakovitch, *Appl. Catal. A: Gen.* **2009**, *360*, 145–153.
- [46] Y. Kitamura, S. Sako, A. Tsutsui, Y. Monguchi, T. Maegawa, Y. Kitade, H. Sajiki, *Adv. Synth. Catal.* **2010**, *352*, 718–730.
- [47] S. S. Soomro, F. L. Ansari, K. Chatziapostolou, K. Köhler, *J. Catal.* **2010**, *273*, 138–146.
- [48] L. Joucla, G. Cusati, C. Pinel, L. Djakovitch, *Adv. Synth. Catal.* **2010**, *352*, 1993–2001.
- [49] Y. Wang, H. Liu, *J. Mol. Catal.* **1988**, *45*, 127–142.
- [50] L. Djakovitch, K. Koehler, *J. Mol. Catal. A: Chem.* **1999**, *142*, 275–284.
- [51] J. Schwarz, V. P. W. Bohm, M. G. Gardiner, M. Grosche, W. A. Herrmann, W. Hieringer, G. Raudaschl-Sieber, *Chem. Eur. J.* **2000**, *6*, 1773–1780.
- [52] M. Wagner, K. Köhler, L. Djakovitch, S. Weinkauff, V. Hagen, M. Muhler, *Top. Catal.* **2000**, *13*, 319–326.
- [53] F. Zhao, B. M. Bhanage, M. Shirai, M. Arai, *Chem. Eur. J.* **2000**, *6*, 843–848.
- [54] F. Zhao, K. Murakami, M. Shirai, M. Arai, *J. Catal.* **2000**, *194*, 479–483.
- [55] J. H. Clark, D. J. Macquarrie, E. B. Mubofu, *Green Chem.* **2000**, *2*, 53–55.
- [56] L. Djakovitch, K. Koehler, *J. Am. Chem. Soc.* **2001**, *123*, 5990–5999.
- [57] K. Köhler, M. Wagner, L. Djakovitch, *Catal. Today* **2001**, *66*, 105–114.
- [58] K. Köhler, R. G. Heidenreich, J. G. E. Krauter, J. Pietsch, *Chem. Eur. J.* **2002**, *8*, 622–631.
- [59] R. G. Heidenreich, J. G. E. Krauter, J. Pietsch, K. Köhler, *J. Mol. Catal. A: Chem.* **2002**, *182–183*, 499–509.
- [60] L. Djakovitch, M. Wagner, C. G. Hartung, M. Beller, K. Koehler, *J. Mol. Catal. A: Chem.* **2004**, *219*, 121–130.
- [61] K. Q. Yu, W. Sommer, M. Weck, C. W. Jones, *J. Catal.* **2004**, *226*, 101–110.
- [62] S. S. Pröckl, W. Kleist, M. A. Gruber, K. Köhler, *Angew. Chem.* **2004**, *116*, 1917–1918; *Angew. Chem. Int. Ed.* **2004**, *43*, 1881–1882.
- [63] J. Horniakova, T. Raja, Y. Kubota, Y. Sugi, *J. Mol. Catal. A: Chem.* **2004**, *217*, 73–80.
- [64] A. Papp, K. Miklos, P. Forgo, A. Molnar, *J. Mol. Catal. A: Chem.* **2005**, *229*, 107–116.
- [65] K. Q. Yu, W. Sommer, J. M. Richardson, M. Weck, C. W. Jones, *Adv. Synth. Catal.* **2005**, *347*, 161–171.

- [66] Y. Y. Ji, S. Jain, R. J. Davis, *J. Phys. Chem. B* **2005**, *109*, 17232–17238.
- [67] K. Okumura, K. Nota, K. Yoshida, M. Niwa, *J. Catal.* **2005**, *231*, 245–253.
- [68] S. Noël, C. Luo, C. Pinel, L. Djakovitch, *Adv. Synth. Catal.* **2007**, *349*, 1128–1140.
- [69] J. Zhu, T. Zhao, I. Kvande, D. Chen, X. Zhou, W. Yuan, *Chin. J. Catal.* **2008**, *29*, 1145–1151.
- [70] B. Tamami, S. Ghasemi, *J. Mol. Catal. A: Chem.* **2010**, *322*, 98–105.
- [71] J. Tarabay, W. Al-Maksoud, F. Jaber, C. Pinel, S. Prakash, L. Djakovitch, *Appl. Catal. A: Gen.* **2010**, *388*, 124–133.
- [72] N. Batail, A. Bendjeriou, L. Djakovitch, V. Dufaud, *Appl. Catal. A: Gen.* **2010**, *388*, 179–187.
- [73] V. Dufaud, F. Beauchesne, L. Bonneviot, *Angew. Chem.* **2005**, *117*, 3541–3543; *Angew. Chem. Int. Ed.* **2005**, *44*, 3475–3477.
- [74] A. Alimardanov, L. Schmieder-van de Vondervoort, A. H. M. de Vries, J. G. de Vries, *Adv. Synth. Catal.* **2004**, *346*, 1812–1817.
- [75] J. G. De Vries, *Dalton Trans.* **2006**, 421–429.
- [76] M. T. Reetz, J. G. de Vries, *Chem. Commun.* **2004**, *0*, 1559–1563.
- [77] L. Djakovitch, K. Koehler, J. G. De Vries, in: *Nanoparticles and Catalysis*, (Ed.: D. Astruc), Wiley-VCH, Weinheim, **2008**, pp 303–348.
- [78] Y. Yang, J. Q. Guan, P. P. Qiu, Q. B. Kan, *Appl. Surf. Sci.* **2010**, *256*, 3346–3351.
- [79] A. Chica, A. Corma, M. E. Domine, *J. Catal.* **2006**, *242*, 299–308.
- [80] S. Krijnen, H. C. L. Abbenhuis, R. W. J. M. Hanssen, J. H. C. van Hooff, R. A. van Santen, *Angew. Chem.* **1998**, *110*, 374–376; *Angew. Chem. Int. Ed.* **1998**, *37*, 356–358.
- [81] C.-M. Andersson, K. Karabelas, A. Hallberg, *J. Org. Chem.* **1985**, *50*, 3891–3895.
- [82] D. E. Bergbreiter, A. M. Kippenberger, G. Tao, *Chem. Commun.* **2002**, 2158–2159.
- [83] M. T. Reetz, E. Westermann, *Angew. Chem.* **2000**, *112*, 170–173; *Angew. Chem. Int. Ed.* **2000**, *39*, 165–168.

**14** Carbonylative Sonogashira Coupling in the Synthesis of Ynone: A Study of “Boomerang” Phenomena

*Adv. Synth. Catal.* **2013**, 355, 1–14

Marie Genelot, Véronique Dufaud,\* Laurent Djakovitch\*

